Proceedings of the
9th Graz Brain-Computer Interface Conference 2024

10.3217/978-3-99161-014-4-014

CORRECTING TRAJECTORY-DECODING ERRORS VIA CORTICAL SUBSTRATES OF CONTINUOUS ERRONEOUS FEEDBACK PROCESSING

H.S. Pulferer[1], K. Kostoglou[1], N. Srisrisawang[1], G.R. Müller-Putz[1,2]

[1]Institute of Neural Engineering, Graz University of Technology, Graz, Austria
[2]BioTechMed-Graz, Graz, Austria

E-mail: gernot.mueller@tugraz.at

ABSTRACT: Decades of research thoroughly established various neural correlates of processing *discrete errors*, i.e., events that may be classified as either *correct* or *wrong*. However, despite many successful demonstrations of brain-computer interfaces (BCIs) utilizing these discrete correlates, a range of everyday tasks (e.g., car driving) requires fine-tuned feedback control that already transgresses such coarse distinction. Following up on recent research in the field of *continuous* erroneous feedback processing, we propose the regression of *continuous feedback-target deviations* from the electroencephalogram (EEG). Within thirty pre-recorded sessions of data in ten participants, employing a 2D target-tracking task that offered online feedback, we thus utilized a convolutional neural network to infer ongoing feedback-target deviations and correct the feedback's position accordingly in an offline evaluation. The presented correction approach significantly improved correlations between feedback and target kinematics - a first indication that *continuous* error-related cortical activity can be utilized in BCIs as well.

INTRODUCTION

Over the last thirty years, a large body of research extensively documented the cortical response to discrete erroneous stimuli [1, 2]. In this context, the error-related negativity (ERN) and error positivity (Pe) – frontocentral and centroparietal deflections in the scalp potentials, respectively – quickly emerged as two key markers for error processing and error awareness [3, 4]. Arising approximately 100ms (ERN) and 300-500ms (Pe) after an erroneous stimulus, the sequence of these two potentials was termed the *error-related potential* (ErrP) and met increasing interest as a control signal within the field of brain-computer interfaces (BCIs) [5–7]. However, while various approaches emerged to utilize the ErrP as a control signal - seeking, e.g., to prevent the execution of erroneous commands altogether, or recalibrate the interface in response to errors [5] - a number of issues surrounding the discrete correlates to error processing persist.

For one, the neurophysiology of the ErrP proved notably sensitive to a range of factors. Advanced age [8], lowered levels of attention [9], or reduced attributed significance to an error [10] reportedly alter the measured potentials, leading to corresponding difficulties in BCI operation [11]. Furthermore – and arguably the biggest limitation to utilizing ErrPs for BCI applications – the presence or absence of the ErrP intrinsically encodes binary information only. However, various tasks such as car driving or moving a cursor on-screen demand minute adjustments depending on the perceived discrepancy between intention and outcome rather than a coarse distinction into *error* or *no error*.

While some literature already attempted an expansion to continuous error processing within BCIs, this predominantly encompassed the presentation of discrete stimuli in a continuous paradigm [12–15]. Recent work by our group first reported the occurrence of cortical modulations with continuous feedback-target deviations [16], however, the usefulness of this neural substrate within BCIs remains to be established.

In this work, we thus aimed to close the gap in knowledge and answer two major questions. First, is it possible to regress target-feedback discrepancies from neural markers of continuous erroneous feedback processing within the electroencephalogram (EEG)? And second, can these inferences be used to subsequently correct the initial feedback and alleviate the feedback-target mismatch? Using thirty sessions of previously recorded data of an online target-tracking task with different feedback conditions, we trained a convolutional neural network (CNN) to infer the discrepancy (error signal) between feedback and target position in two spatial dimensions from the EEG. We then adjusted the recorded feedback trajectories as decoded and presented during the online measurements by the inferred error signal to obtain *corrected feedback trajectories*. Compared to the recorded feedback trajectories, correlations with the target trajectories significantly improved for the corrected feedback trajectories, indicating notable merit to using neural signatures of continuous erroneous feedback processing for automated correction of interface-related errors within a BCI.

MATERIALS AND METHODS

Dataset: The prerecorded dataset [17] consisted of the 60-channel EEG (10-10 electrode system) and 4-channel electrooculogram (EOG) of ten able-bodied,

Published by
Verlag der Technischen Universität Graz

10.3217/978-3-99161-014-4-014

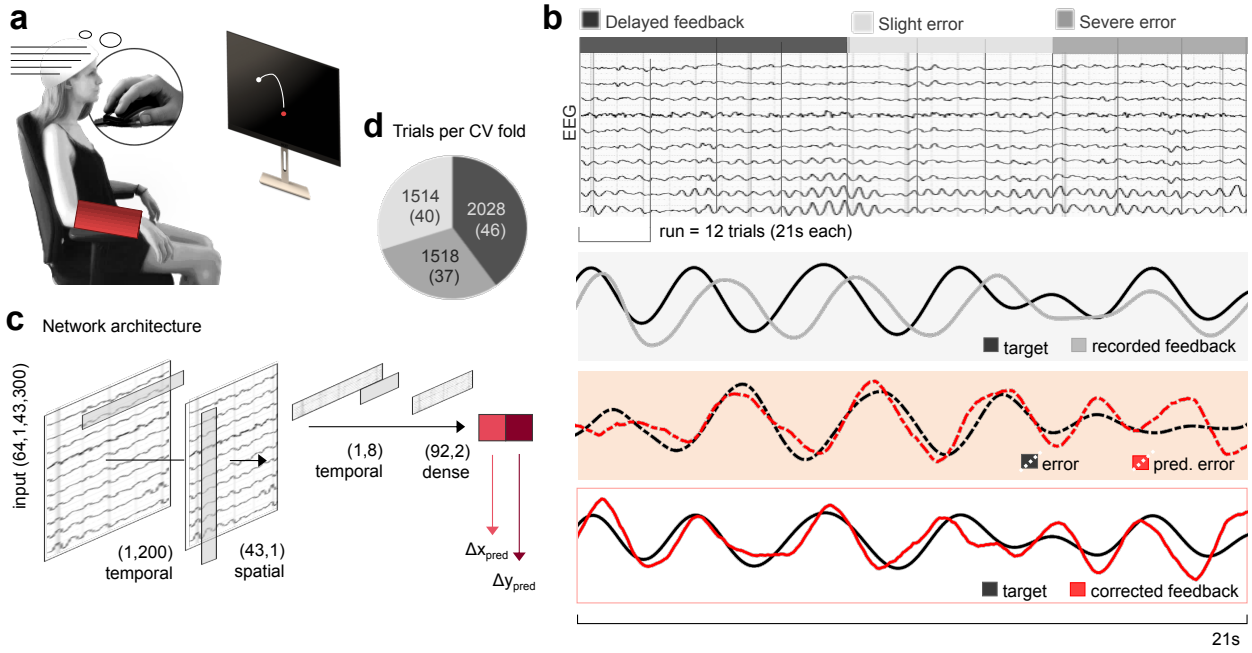

Figure 1: **(a)** Experimental setup. Participants attempted cursor-like movement of their strapped dominant arm to trace a moving object on-screen (snake, white) with real-time feedback (red dot). **(b)** Feedback conditions and approach. Target and feedback kinematic (grey box), as well as EEG, were previously recorded within the three different feedback conditions Delayed feedback, *Slight error*, and *Severe error*. Distances in x and y between recorded target and feedback trajectories are calculated as error signals (red box) and predicted from a convolutional neural network **(c)**. Corrected feedback trajectories are obtained from initial feedback and decoded error signals (red framed box). **(d)** Average number and standard deviation of available trials per cross-validation fold for each participant and session (training: 4 folds, validation: 1 fold, testing: 1 fold). Exemplary trajectories for the correction approach in **(b)** are taken from session 1 of participant P2 (y coordinate, Slight error condition).

right-handed participants in total of 30 sessions, sampled at 200Hz. The dataset was chosen due to previously unveiled cortical modulations with the ongoing target-feedback deviations [16], indeed suggesting error-related brain activity elicited within the employed task.

Paradigm: During each session of this previously recorded online study, participants *attempted* cursor-like movement as if wielding a computer mouse to track a moving target on-screen (*snake*). An encasing around their dominant arm (see Fig.1a) limited overt movement. Utilizing a combination of partial least squares regression and an unscented Kalman filter (PLSUKF) [18], estimates for the snake's trajectory were decoded in real time from the EEG and delivered within different feedback conditions in the form of a feedback dot on-screen. Each participant underwent three separate sessions of measurements within the time span of a week. The multiple sessions (each employing the identical paradigm conditions) were initially designed to evaluate session-to-session differences in performance; as no significant changes were found in the initial work [17], we disregarded the session information and pooled all data to a total of 30 sessions for the current work.

Feedback conditions: Each session commenced with four calibration runs, followed by three 50% and three 100% EEG-decoded online feedback runs (see Fig.1b). One run comprised 12 trials of 23s length, respectively, during which participants tracked the moving snake on-screen. The first and last second in each run were omitted from further analysis to further minimize movement-related artifacts as the participants became aware of the start and end of each run, leading to 21s of data per run.
Within the calibration runs, EEG data to fit the PLSUKF online-decoder was recorded; as such, no EEG-decoded trajectory information was available yet to display as feedback. To accustom the participants to the additional visual input of the feedback dot from the beginning nonetheless, *fake feedback* in the form of a slightly delayed snake was presented during the calibration runs. As feedback dot and snake largely coincided throughout the calibration runs, leading to minimal discrepancy between target and feedback, calibration runs are henceforth termed *Delayed feedback*.
After fitting the PLSUKF decoder with the calibration data, the measurement proceeded with *online* EEG-decoded feedback. To transition smoothly between fake and online-decoded feedback, three intermediate 50% EEG-decoded feedback runs were introduced, wherein the arithmetic mean between actual (snake) and EEG-decoded target positions was displayed. Due to the EEG-decoded information, the discrepancy between target and feedback increased notably with respect to the calibration runs. We thus term the 50% EEG-decoded feedback runs *Slight error* in the following.
In the final three runs, 100% EEG-decoded feedback was displayed. In contrast to the mixed information shown during the 50% EEG-decoded feedback runs, participants were now faced with considerable discrepancy between target and feedback due to limitations in decoding. We thus term the 100% EEG-decoded feedback runs *Severe*

Published by
Verlag der Technischen Universität Graz

10.3217/978-3-99161-014-4-014

error in the following.

Data processing: Both EEG and EOG data were bandpass filtered between 0.2-10Hz (10th order Butterworth). Subsequently, noisy channels of the EEG as identified during the online experiment were spherically interpolated from neighboring channels. Eye artifacts were similarly attenuated utilizing the stored correction matrices of the SGEYESUB algorithm [19] from the online measurement, after which the EOG channels were removed. Persistent eye artifacts as well as muscle artifacts at peripheral EEG channels were identified via independent component analysis (ICA) and removed. To further eliminate any eye- or muscle-related influence, the outermost EEG channels (i.e., positions AF7-AF8, F7/8, FT7/8, T7/8, TP7/8, P7/8, PO7/8) were excluded from our analysis scheme, leading to a remaining number of 43 EEG channels.

The recorded x and y coordinates of the target (snake), as well as of the displayed feedback dot, were smoothed using a Savitzky-Golay filter (second order polynomials, 21 sample window ∼100ms). The distance vector $\vec{\Delta}(t)$ between feedback (fb) and target (tg) position in each time point t, i.e., the *error signal* in two dimensions, was then derived via:

$$\vec{\Delta}(t) = \vec{X}(t)_{fb} - \vec{X}(t)_{tg} \in \mathbb{R}^2. \quad (1)$$

Neural network architecture: The aim of this work was to utilize the continuous error-related brain activity representing the ongoing target-feedback discrepancy to *correct* the initially recorded EEG-decoded predictions for the target position. To this end, we modified EEGNet [20] and changed the output layer to simultaneously regress the x and y coordinates of the error signal ($\vec{\Delta}$) from 300-sample windows of EEG data (i.e., 1.5s). Importantly, several other architectures, such as Deep ConvNet [21] or EEG-TCNet [22], could have been employed as well; as the current study however mainly corresponds to a proof of concept, benchmarking has not been undertaken in the scope of this work.

In detail, the utilized network consisted of three layers. Within the first layer, the temporal dimension of the input frames was zero-padded (75 samples at both edges) and temporally convolved in 16 filters to extract temporal features from the EEG (kernel size (1,200)). The large kernel size corresponding to a 1s window was chosen to enable the model to learn from frequency information down to 1Hz, as previous findings revealed contributions of predominantly the delta band for the used dataset [16]. In the second layer, a consecutive depthwise convolution (kernel size (43,1)) extracted spatial features in 8 filters by condensing the information of all considered channels to one single value, followed by subsequent temporal average pooling (kernel size (1,4)). In the final third layer, a second temporal convolution in 4 filters was employed (kernel size (1,16)), followed by average pooling (kernel size (1,2)). Each mentioned convolutional layer was followed by batch normalization to accelerate convergence [23], as well as dropout to impede an overfit on the training data (rates of 0.25, 0.35, and 0.45 for 1st, 2nd and 3rd layer). For activation functions in each neuron, exponential linear units were used [24]. Finally, the outputs of the third layer were flattened and passed through a fully connected layer (92 input features, 2 output features), returning the 2D prediction $\vec{\Delta}_{pred}$ of the error signal. For each batch, the predictions were smoothed with a Savitzky-Golay filter to alleviate noise (2nd order polynomials, 21 samples). All network models were implemented, trained and evaluated using PyTorch.

Network training procedure and regression performance: For each participant, session, and condition, we sliced the EEG data into windows containing 300 samples with a stride of 15 samples (i.e., 1.5s windows, sampled every 75ms). We retained the last sixth of the resulting windows for testing in a causal fashion, while the optimum model - i.e., the model maximizing the validation correlation (mean of both x and y coordinate) between actual ($\vec{\Delta}$) and predicted ($\vec{\Delta}_{pred}$) error signal - was found via 5-fold cross-validation on the remaining data. For each fold, we trained a model for 30 epochs using a batch size of 64 and a learning rate of 1e-4. Notably, predicting the error signal for 64 consecutive 1.5s-windows at a stride of 75ms per batch lead to 64·0.075s=4.8s-long trajectories of predictions, for which both the correlation and the RMSE values with the ground truth were evaluated. To optimize the model's parameters with respect to the mean squared error loss, we used the Adam optimization algorithm [25]. The overall performance of each regression model was then assessed via Pearson's correlation coefficient, as well as the root mean square error (RMSE) between actual ($\vec{\Delta}$) and predicted ($\vec{\Delta}_{pred}$) error signal within each batch. The overall testing performance then corresponded to the average across all batches within the testing set.

To additionally analyze each EEG channel's contribution to the regression performance, we iteratively set one of the 43 channels within the testing data to zero (i.e., we simulated one dead channel at a time) and reevaluated the regression performance. The absolute difference between the optimum model's testing performance and the dead-channel performance for each removed channel then provided an estimate for the specific channel's importance.

Trajectory correction and correction performance: Utilizing the prediction $\vec{\Delta}_{pred}$ of the error signal acquired via the neural network (Fig.1c), we obtained *corrected feedback trajectories* (i.e., new target predictions[1]) via Equ.(1) as:

$$\vec{X}_{fb,corr} = \vec{X}_{fb} - \vec{\Delta}_{pred} = \vec{X}_{tg,pred} \in \mathbb{R}^2. \quad (2)$$

The overall merit of our correction approach was judged by comparing Pearson's correlation coefficients and the RMSE values between a) target and recorded feedback

[1] Note that from the relation in Equ.(2), we indeed gain *target predictions*. However, to keep consistent terminology (the recorded feedback $\vec{X}_{fb}$ depicted during the measurement corresponded to target predictions as well, if from the PLSUKF regressor), we term these new target predictions *corrected feedback*.

Published by
Verlag der Technischen Universität Graz

10.3217/978-3-99161-014-4-014

(i.e., $\vec{X}_{tg}$ and $\vec{X}_{fb}$) and b) target and corrected feedback (i.e., $\vec{X}_{tg}$ and $\vec{X}_{fb}$,corr).

Chance level estimation: To establish whether the network models truly discern cortical activity rather than noise, we estimated individual chance levels for the regression performance in each participant, session, and condition. To this end, we randomly shuffled the target information (i.e., the error signal $\vec{\Delta}$) across batches of testing data, effectively breaking any causal relation between brain activity and corresponding target-feedback discrepancy without changing the frequency content of $\vec{\Delta}$ (equivalently, the input signals could have been shuffled as well, leading however to the same results at a higher computational cost). The previously trained optimum model for the corresponding participant, session, and condition was then evaluated on the shuffled data. This approach was repeated for 100 times, yielding a chance distribution of correlations and RMSE values between actual ($\vec{\Delta}$) and predicted ($\vec{\Delta}_{pred,shuff}$) error signals. The chance levels for the correlations and RMSE values within each regression model were then identified as the 95th and 5th percentiles of the corresponding chance distributions, respectively.

We further investigated the nature of possible improvements in correlations and RMSE values due to our approach in Equ.(2). Specifically, improvements in correlation or RMSE values between target and corrected feedback (i.e., $\vec{X}_{tg}$ and $\vec{X}_{fb,corr}$) compared to those between target and recorded feedback (i.e., $\vec{X}_{tg}$ and $\vec{X}_{fb}$) may merely correspond to spurious fluctuations in performance due to the addition of the smoothed (low-frequency) predictions to the recorded feedback. To eradicate this concern, we once more exploited the previously outlined shuffling approach. We randomly shuffled the pairs of recorded target and feedback information across batches, breaking all causal relations with the EEG input while retaining the temporal structure within each batch. The optimum model then predicted the error signals $\vec{\Delta}_{pred}$, which in turn served to obtain randomly corrected feedback trajectories according to Equ.(2). The shuffling was repeated for 100 times, yielding chance distributions for the correlation and RMSE values between target ($\vec{X}_{tg}$) and randomly corrected feedback ($\vec{X}_{fb,corr,shuff}$) trajectories. The chance levels for the correlations and RMSE values within the correction approach for each participant, session, and condition were then found as the 95th and 5th percentiles of the chance distributions, respectively.

Table (1) summarizes all utilized evaluation approaches.

Table 1: Summary of evaluation approaches

Assessment	Correlation/RMSE between
Regression *performance*	$\vec{\Delta}, \vec{\Delta}_{pred}$
Regression *chance level*	$\vec{\Delta}, \vec{\Delta}_{pred,shuff}$ (p95 for correlation, p5 for RMSE)
Correction *performance*	$\vec{X}_{tg}, \vec{X}_{fb,corr}$ compared to $\vec{X}_{tg}, \vec{X}_{fb}$
Correction *chance level*	$\vec{X}_{tg}, \vec{X}_{fb,corr,shuff}$ (p95 for correlation, p5 for RMSE)

RESULTS

Regression performance: Individual CNN models were trained for each participant, session and condition; the overall regression performance for each feedback condition is outlined in Fig.2(a-b). The single dots correspond to the 30 sessions (pooling all three sessions per participant in the 10 participants); mean and median are displayed as dashed and solid lines within the boxes, respectively, solid black lines denote the corresponding chance levels.

On average, we obtained mean correlations across both coordinates of 0.36, 0.32 and 0.23 between actual ($\vec{\Delta}$) and predicted ($\vec{\Delta}_{pred}$) error signals for Delayed feedback, Slight error and Severe error conditions, each of which ranges above the corresponding chance level (approximately 0.15, 0.17 and 0.17). Similarly, the observed mean RMSE values across both coordinates of 56px, 106px and 187px for Delayed feedback, Slight error and Severe error condition cut beneath their corresponding chance levels (64px, 115px and 193px; see Fig.2b).

Notably, the regression performance worsened for both metrics with increasing discrepancy between target and feedback (note the different scales). In this context, our feature analysis unveiled growing scalp regions of importance across feedback conditions, displaying increasing central and parietooccipital engagement as the feedback deviates from the target (see Fig.2(e)). Left (bright) and right (dark) topographical maps correspond to the most relevant EEG channels for predicting x and y coordinate of the error signal $\vec{\Delta}$, respectively.

Correction performance: The mean correction performance due to our approach is displayed in the white panel of Fig.2. Light and dark gray results correspond to the x and y coordinate results pertaining to the recorded feedback ($\vec{X}_{fb}$); light and dark red display the x and y coordinate results for the corrected feedback ($\vec{X}_{fb,corr}$).

A right-tailed paired Wilcoxon signed rank test, Bonferroni-corrected for six tests (three conditions in two coordinates), revealed significantly higher correlations with the target trajectories ($\vec{X}_{tg}$) for our corrected feedback trajectories ($\vec{X}_{fb,corr}$) compared to the recorded ones ($\vec{X}_{fb}$) (see Fig.2(c); significance levels of 0.05, 0.01, and 0.001 are marked as *, **, and ***).

Overall, we observed an average improvement in correlation across both coordinates of approximately 0.03, 0.07, and 0.08 for Delayed feedback, Slight error, and Severe error conditions due to the feedback correction; however, only the corrections for the first two conditions range on average above chance. In terms of RMSE values, significant differences arose only for the Delayed feedback condition and one coordinate within the Slight error condition, even though all mean values fell beneath the chance levels (see Fig.2(d)).

DISCUSSION AND CONCLUSION

Published by
Verlag der Technischen Universität Graz

10.3217/978-3-99161-014-4-014

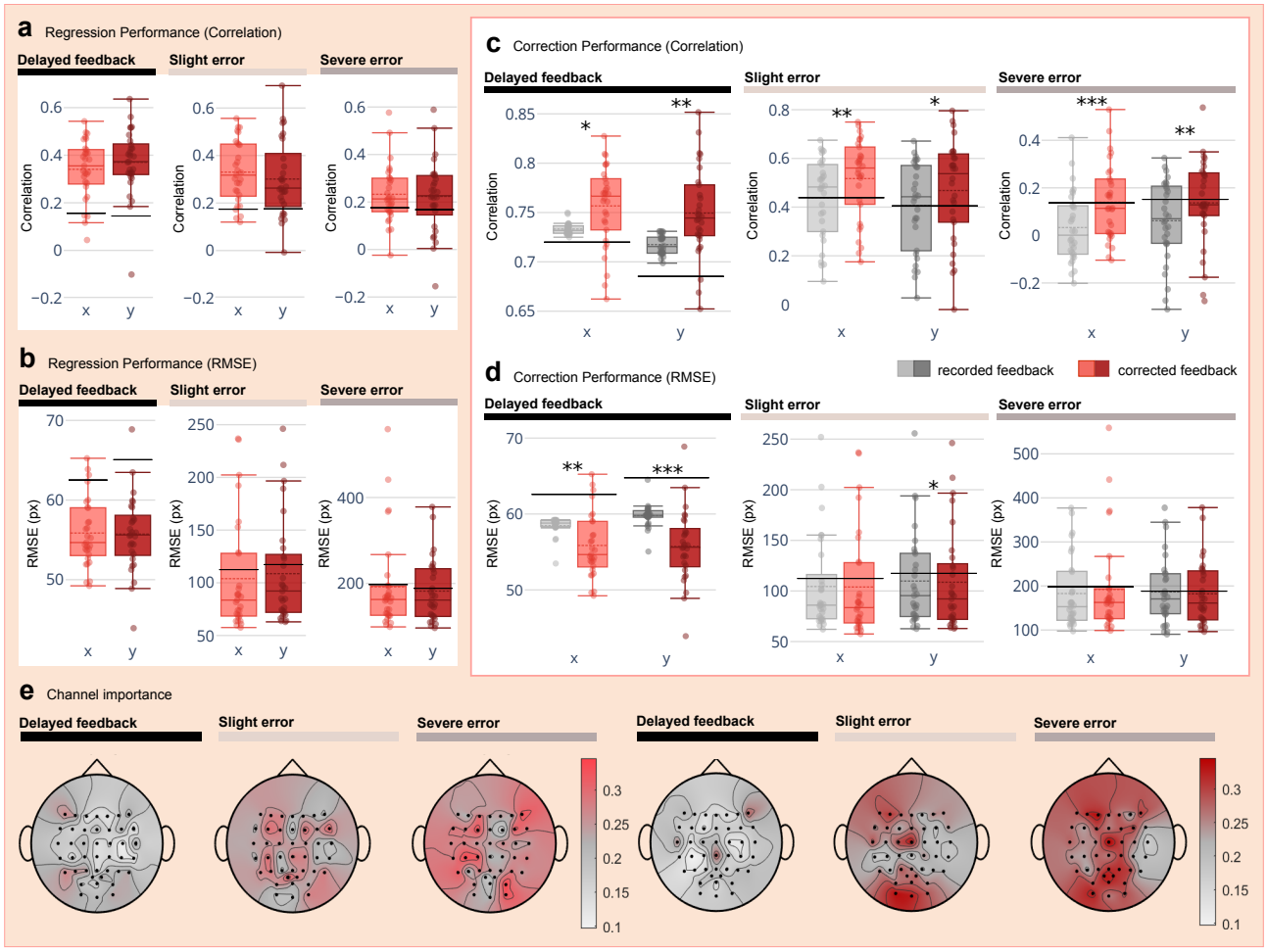

Figure 2: **(a-b)** Correlations and RMSE values between actual and decoded error signal as obtained by the CNN-regression. Bright and dark red color indicate results in the x and y coordinate, respectively. **(c-d)** Correlations and RMSE values for the correction approach. Measures between target and recorded feedback trajectories are shown in gray, measures between target and corrected feedback trajectories in red. Bright and dark colors indicate results in the x and y coordinate. For all box plots, single session means are depicted as dots, dashed and solid lines denote mean and median of the distributions, respectively. Black horizontal lines indicate the corresponding chance levels. **(e)** Averaged normalized channel importance maps for the error signal regression as obtained by setting one channel at a time to zero and evaluating the resulting drop in performance. Left and right topographical maps correspond to the importance in predicting the x and y coordinate of $\vec{\Delta}$, respectively.

Within the offline analysis of 30 sessions of EEG recordings, we present a first attempt at correcting previously inferred feedback trajectories during a target tracking task by utilizing markers for continuous erroneous feedback processing within the brain.

Using an adaption of the well-known neural network architecture of EEGNet, we presented evidence for the successful inference of continuous feedback-target deviations (*error signals*) from the EEG for the first time. Achieving mean correlations with the actual error signals of between 0.23 and 0.36 for the investigated conditions (Fig2(a)), the obtained predictions proved to range above chance level, indicating that the regression of this type of error-related information from the EEG is indeed feasible.

Interestingly, the regression performance peaked within the only minor deviations during the Delayed feedback condition and dropped steadily across conditions with increasing feedback-target deviation. However, previous neurophysiological findings for the used dataset indicated an opposing effect, e.g., increasingly prominent cortical modulations with increasing absolute distance from the target [16]. While the obtained channel importance maps affirm the previous findings with the emergence of increasing central and centrooccipital relevance with increasing error severity and indeed indicate that the models learned from error-related features, our overall results might suggest that the error signal's x and y components are not sufficiently encoded within the brain. Future approaches will have to clarify whether better performance could be achieved by taking the modulus, i.e., the Euclidean distance between feedback and target, into account; possible implementations could for example switch to radial coordinates or add the error signal's modulus to the network's training procedure.

Despite the moderate correlations for the regression itself, the correction approach nonetheless proved to be of merit. We observed significant improvements in correlations with the target trajectories for our corrected feedback compared to the initially recorded feedback trajectories across all feedback conditions. A chance level evaluation certified these improvements as better

Published by
Verlag der Technischen Universität Graz

10.3217/978-3-99161-014-4-014

than random for all but the Severe error condition. However, for this condition, initial correlations between recorded target and feedback trajectories already failed to meet the chance level, which could be improved considerably due to our approach nonetheless.
In summary, we conclude that the use of continuous error-related brain activity can significantly improve the performance of a BCI and that further work in this field will be of great value for future implementations.

ACKNOWLEDGMENTS
The authors thank the extended Graz BCI team, especially Adyasha Dash, for valuable comments. Research was supported by the NTU-TUG Joint Ph.D. Program.

REFERENCES

[1] Falkenstein, Hohnsbein, Hoormann, Blanke. Error processing in choice reaction tasks with focused and crossmodal divided attention. an ERP study. l Conference on EventRelated Potenti als of the Brain. May 23-June 3, Noordwijk, the Netherlands. 1989.
[2] Gehring WJ. The error-related negativity: Evidence for a neural mechanism for error-related processing. University of Illinois at Urbana-Champaign (1992).
[3] Nieuwenhuis S, Ridderinkhof KR, Blom J, Band GP, Kok A. Error-related brain potentials are differentially related to awareness of response errors: Evidence from an antisaccade task. Psychophysiology. 2001;38(5):752–760.
[4] Holroyd CB, Nieuwenhuis S, Mars RB, Coles MGH. Anterior cingulate cortex, selection for action, and error processing. In: Cognitive neuroscience of attention (pp. The Guilford Press, xiii: New York, NY, US, 2004, 219–231.
[5] Chavarriaga R, Sobolewski A, Millán JDR. Errare machinale est: The use of error-related potentials in brain-machine interfaces. Front. Neurosci.. 2014;8:208.
[6] Müller-Putz GR *et al.* Feel your reach: An EEG-based framework to continuously detect goal-directed movements and error processing to gate kinesthetic feedback informed artificial arm control. Frontiers in Human Neuroscience. 2022:110.
[7] Wimmer M, Weidinger N, Veas E, Müller-Putz GR. Multimodal decoding of error processing in a virtual reality flight simulation. Sci. Rep.. 2024;14(1):1–14.
[8] Falkenstein M, Hoormann J, Hohnsbein J. Changes of error-related ERPs with age. Exp. Brain Res.. 2001;138(2):258–262.
[9] Yeung N, Botvinick MM, Cohen JD. The neural basis of error detection: Conflict monitoring and the error-related negativity. Psychol. Rev.. 2004;111(4):931–959.
[10] Hajcak G, Moser JS, Yeung N, Simons RF. On the ERN and the significance of errors. Psychophysiology. 2005;42(2):151–160.
[11] Chavarriaga R, Millan JDR. Learning from EEG error-related potentials in noninvasive brain-computer interfaces. IEEE Trans. Neural Syst. Rehabil. Eng.. 2010;18(4):381–388.
[12] Zhang H, Chavarriaga R, Khaliliardali Z, Gheorghe L, Iturrate I, Millán JdR. EEG-based decoding of error-related brain activity in a real-world driving task. J. Neural Eng.. 2015;12(6):066028.
[13] Lopes-Dias C, Sburlea AI, Müller-Putz GR. Online asynchronous decoding of error-related potentials during the continuous control of a robot. Sci. Rep.. 2019;9(1):17596.
[14] Wimmer, Weidinger, ElSayed, Müller-Putz, Veas. EEG-Based error detection can challenge human reaction time in a VR navigation task. In: 2023 IEEE International Symposium on Mixed and Augmented Reality (ISMAR). Oct. 2023, 970–979.
[15] Mondini V, Sburlea AI, Müller-Putz GR. Towards unlocking motor control in spinal cord injured by applying an online EEG-based framework to decode motor intention, trajectory and error processing. Sci. Rep.. 2024;14(1):4714.
[16] Pulferer HS, Kostoglou K, Müller-Putz GR. Getting off track: Cortical feedback processing network modulated by continuous error signal during target-feedback mismatch. Neuroimage. 2023;274:120144.
[17] Pulferer HS, Ásgeirsdóttir B, Mondini V, Sburlea AI, Müller-Putz GR. Continuous 2D trajectory decoding from attempted movement: Across-session performance in able-bodied and feasibility in a spinal cord injured participant. J. Neural Eng.. 2022.
[18] Mondini V, Kobler RJ, Sburlea AI, Müller-Putz GR. Continuous low-frequency EEG decoding of arm movement for closed-loop, natural control of a robotic arm. J. Neural Eng.. 2020;17(4):046031.
[19] Kobler RJ, Sburlea AI, Lopes-Dias C, Schwarz A, Hirata M, Müller-Putz GR. Corneo-retinal-dipole and eyelid-related eye artifacts can be corrected offline and online in electroencephalographic and magnetoencephalographic signals. Neuroimage. 2020;218:117000.
[20] Lawhern VJ, Solon AJ, Waytowich NR, Gordon SM, Hung CP, Lance BJ. EEGNet: A compact convolutional neural network for EEG-based brain-computer interfaces. J. Neural Eng.. 2018;15(5):056013.
[21] Schirrmeister RT *et al.* Deep learning with convolutional neural networks for EEG decoding and visualization. Hum. Brain Mapp.. 2017;38(11):5391–5420.
[22] Ingolfsson TM, Hersche M, Wang X, Kobayashi N, Cavigelli L, Benini L. EEG-TCNet: An accurate temporal convolutional network for embedded Motor-Imagery Brain–Machine interfaces. In: 2020 IEEE International Conference on Systems, Man, and Cybernetics (SMC). IEEE, Oct. 2020, 2958–2965.
[23] Ioffe S, Szegedy C. Batch normalization: Accelerating deep network training by reducing internal covariate shift. 2015.
[24] Clevert DA, Unterthiner T, Hochreiter S. Fast and accurate deep network learning by exponential linear units (ELUs). 2015.
[25] Kingma DP, Ba J. Adam: A method for stochastic optimization. 2014.

Published by
Verlag der Technischen Universität Graz